In Situ Scanning Tunneling Microscopy of Benzene Adsorbed on Rh(111) and Pt(111) in HF Solution

Shueh-Lin Yau, Youn-Geun Kim, and Kingo Itaya*

Contribution from the Itaya Electrochemiscopy Project, ERATO/JRDC, Research Institute of Electric and Magnetic Materials, Yagiyama-Minami 2-1-1, Sendai, Japan 982, and Department of Applied Chemistry, Faculty of Engineering, Tohoku University, Sendai, Japan 982

Received March 19, 1996[⊗]

Abstract: Adsorption of benzene on well-ordered Rh(111) and Pt(111) electrodes was investigated in HF solution using in situ scanning tunneling microscopy (STM). Ordered adlayers of adsorbed benzene with a *c*(2$\sqrt{3}$ × 3)-*rect*-2C_6H_6 (θ = 0.17) symmetry were found to form on both electrodes in the double-layer charging region. A phase transition was observed in the benzene adlayer at negative potentials, where partial desorption of adsorbed benzene took place. The *c*(2$\sqrt{3}$ × 3)*rect* structure was transformed into (3 × 3)-1C_6H_6 (θ = 0.11) and ($\sqrt{21}$ × $\sqrt{21}$)*R*10.9° (θ = 0.14) on Rh(111) and Pt(111), respectively. High-resolution STM images obtained on Rh(111) revealed the internal structures of benzene molecules adsorbed at different binding sites in both phases. They appeared as triangular and dumbbell shapes in the (3 × 3) and *c*(2$\sqrt{3}$ × 3)*rect* structures, respectively, implying their 3-fold and 2-fold registries. The 2-fold bridging coordination was thought to occur in the ($\sqrt{21}$ × $\sqrt{21}$)*R*10.9° phase on Pt(111).

Introduction

Adsorption of organic molecules onto electrode surfaces in electrolyte solutions under potential control has a long history for elucidating the roles of structures and properties of adsorbed molecules.[1−3] Although conventional electrochemical and optical techniques such as infrared, Raman, and second harmonic generation (SHG) spectroscopies have been intensively applied to investigate the molecular adsorption at electrode surfaces in solution,[1] they can usually only provide averaged information on the molecular orientation and packing within an adlayer. Ex situ techniques such as low-energy electron diffraction (LEED) and Auger electron spectroscopy (AES) using an ultrahigh vacuum−electrochemical (UHV-EC) technique have also been extensively employed for understanding the relationship between the adsorbed molecules and the surface atomic structure of the electrodes.[2,3] More recently, scanning tunneling microscopy (STM) has been well-recognized as an important in situ method for structural investigations of adsorbed chemical species on well-defined electrode surfaces in electrolyte solution with atomic resolution.[4] Examples include adsorbed halide,[5−8] sulfate,[9−12] and cyanide[13,14] on Pt, Rh, Au, and Ag electrodes.

Small inorganic species adsorbed on the electrode surface can be visualized relatively easily by in situ STM. Few high-resolution STM images have been reported for organic molecules adsorbed at an electrode−electrolyte interface. A few recent papers have reported in situ STM images with relatively high resolution of DNA bases such as adenine, guanine, and cytosine, and of 2,2′-bipyridine adsorbed on highly ordered pyrolytic graphite as well as on Au(111).[15−17] In our recent papers,[18,19] it was demonstrated that highly ordered molecular arrays of porphyrin, crystal violet, and a linear aromatic molecule were easily formed on iodine-modified Au(111) rather than on bare Au, and they were visualized by in situ STM with near-atomic resolution, revealing packing arrangements and even internal molecular structures in solution.[18,19] Such an extraordinarily high resolution achieved in solution strongly encouraged us to investigate the adsorption of relatively small organic molecules directly attached to the electrode surface in order to understand electrocatalytic activities of noble metals such as Pt and Rh.

On the other hand, voluminous reports describe investigation of the adsorption of aromatics such as benzene and its derivatives on Pt, Rh, Ni, Ir, Ru, and Pd in UHV, which were performed by using various surface sensitive techniques such as LEED, AES, and electron energy-loss spectroscopy (EELS) to evaluate gas phase catalytic reactions such as hydrogenation, dehydrogenation, and dehydrocyclization.[20] In UHV, small molecules such as coadsorbed benzene and CO on Rh(111),[21] naphthalene on Pt(111),[22] copper phthalocyanine on Cu(100),[23] and others[24] have successfully been resolved by STM with their

* To whom correspondence should be addressed at Tohoku University.

⊗ Abstract published in *Advance ACS Abstracts,* August 1, 1996.

(1) Lipkowski, J., Ross, P. N., Eds. In *Adsorption of Molecules at Metal Electrodes*; VCH Publishers: New York, 1992.
(2) Hubbard, A. T. *Chem. Rev.* **1988**, *88*, 633.
(3) Soriaga, M. P. *Prog. Surf. Sci.* **1992**, *39*, 525.
(4) Siegenthaler, H. In *Scanning Tunneling Microscopy II*; Wiesendanger, R., Guntherodt, H.-J., Eds.; Springer-Verlag: New York, 1992; pp 7−49.
(5) Yau, S.-L.; Vitus, C. M.; Schardt, B. C. *J. Am. Chem. Soc.* **1990**, *112*, 3677.
(6) Tanaka, S.; Yau, S-L.; Itaya, K. *J. Electroanal. Chem.* **1995**, *396*, 125.
(7) Gao, X. P.; Weaver, M. J. *J. Am. Chem. Soc.* **1992**, *114*, 8544.
(8) Yamada, T.; Batina, N.; Itaya, K. *J. Phys. Chem.* **1995**, *99*, 8817.
(9) Magnussen, O. M.; Hagebock, J.; Hotlos, J.; Behm, R. J. *Faraday Discuss. Chem. Soc.* **1992**, *94*, 329, 398.
(10) Funtikov, A. M.; Linke, U.; Stimming, U.; Vogel, R. *Surf. Sci.* **1995**, *324*, L343.
(11) Wan, L-J.; Yau, S-L.; Itaya, K. *J. Phys. Chem.* **1995**, *99*, 9507.
(12) Edens, G. J.; Gao, X.; Weaver, M. J. *J. Electroanal. Chem.* **1994**, *375*, 357.
(13) Kim, Y.-G.; Yau, S.-L.; Itaya, K. *J. Am. Chem. Soc.* **1996**, *118*, 393.
(14) Stuhlmann, C.; Villegas, I.; Weaver, M. J. *Chem. Phys. Lett.* **1994**, *219*, 319.
(15) Tao, N. J.; DeRose, J. A.; Lindsay, S. M. *J. Phys. Chem.* **1993**, *97*, 910.
(16) Tao, N. J.; Shi, Z. *J. Phys. Chem.* **1994**, *98*, 1464.
(17) Cunha, F.; Tao, N. J. *Phys. Rev. Lett.* **1995**, *75*, 2376.
(18) Kunitake, M. , Batina, N.; Itaya, K. , *Langmuir* **1995**, *11*, 2337.
(19) Batina, N.; Kunitake, M.; Itaya, K. *J. Electroanal. Chem.* **1996**, *405*, 245.
(20) Somorjai, A. T. *Introduction to Surface Chemistry and Catalysis I*; John Wiley & Sons Inc.: New York, 1994.
(21) Ohtani, H.; Wilson, R. J.; Chiang, S.; Mate, C. M. *Phys. Rev. Lett.* **1988**, *60*, 2398.

S0002-7863(96)00903-1 CCC: $12.00 © 1996 American Chemical Society

distinguishable molecular shapes. Particularly, Weiss and Eigler recently found a binding site dependence of the shape of isolated benzene molecules adsorbed on Pt(111) in UHV at 4 K.[25]

Nevertheless, no in situ STM study has previously been carried out on the adsorption of benzene onto well-defined electrode surfaces in aqueous electrolyte solutions. Here, we describe, for the first time, the adlayer structures of benzene adsorbed on Rh(111) and Pt(111) in HF solutions. High-resolution STM images allowed us to determine the packing arrangement and even the internal structure of each benzene molecule.

Experimental Section

Single-crystal beads of Rh and Pt were made by the crystallization of a molten ball formed at the end of respective pure wires in a hydrogen-oxygen flame.[11,26,27] A laser-beam diffraction method was employed to determine the orientation of each single-crystal bead to expose the (111) plane,[28] which was then mechanically polished with successively finer grade diamond pastes down to 0.05 μm. The mechanically polished electrodes were used for the voltammetric measurement. The single-crystal electrodes were annealed in a hydrogen−oxygen flame and quenched in ultrapure water saturated with hydrogen. The electrode was transferred to an electrochemical cell with a droplet of ultrapure water to protect the surface from contamination.[26−28] A solution of 0.01 M HF was prepared from *ultrapure* HF solution (27 M) from Cica-Merck with Millipore water. An HF solution containing 1 mM benzene was made with spectra-grade benzene (Kanto Chemical Co. Ltd., Tokyo, Japan).

The STM was a Nanoscope III (Digital Instruments, Santa Barbara, CA), which was used with a modified STM cell made with poly-(chlorotrifluoroethylene) as described previously.[13,27] The tunneling tips were prepared by electrochemically etching a W wire with a diameter of 0.25 mm in 1 M KOH by applying a 15 V ac, and they were sealed with transparent nail polish to minimize the faradaic current.[6,11] The tip was then soaked in the electrolyte solution for several hours to remove soluble contaminants before STM measurements were started. All images shown here were taken in the constant-current mode to evaluate corrugation heights of adsorbed benzene molecules. The atomic images of the Rh(111) and Pt(111) substrates with the (1×1) structure as described previously[6,11] were routinely observed in HF solution, suggesting that no contaminant existed on the surface. The (1×1) atomic structure of these surfaces was also used for the accurate determination of the crystal orientation with respect to the STM unit and for the calibration of the piezoelectric tube in $x - y$ directions. The cyclic voltammetry was performed with a Hokudo potentiostat (Tokyo, Japan). The electrochemical cell contained a reversible hydrogen electrode (RHE) in 0.01 M HF and a Pt counter electrode. All electrode potentials are reported with respect to the RHE.

Results and Discussion

I. Adsorption of Benzene on Rh(111). 1. Cyclic Voltammetry. Figure 1 shows cyclic voltammograms (CV) of a Rh(111) electrode in the absence and presence of benzene in 0.01 M HF. In the absence of benzene (Figure 1a), the CV obtained on the well-defined Rh(111) at a scan rate of 5 mV/s exhibited several highly reversible characteristic peaks. Although the overall shape of the CV was similar to that reported previously for Rh(111) in HF solutions,[29] the so-called butterfly peaks at 0.62 V appeared as very sharp spikes superimposed on relatively broad wings on the well-ordered Rh(111). The half-peak width of the butterfly peaks was about 15 mV. In addition, the hydrogen adsorption and desorption reactions were clearly found to split into two almost reversible peaks at 0.18 and 0.15 V. It was noted that the heights and widths of these characteristic peaks depended on the quality of the surface of Rh(111) prepared by the flame-annealing−quenching method described in the Experimental Section. Charge densities of approximately 80 and 220 μC/cm^2 were estimated by the integration of CV for the butterfly peaks at 0.62 V and the peaks for the hydrogen adsorption, respectively. The symmetric appearance in the CV in HF suggests that chloride contamination was minimal in this study. Note that the electrochemistry of Rh(111) in $HClO_4$ is complicated by the electrochemical reduction of perchlorate anions, releasing chloride as a reduction product.[26,29,30] For this reason, HF solution was used exclusively for the present investigation on the adsorption of benzene onto the chloride-free Rh(111) surface.

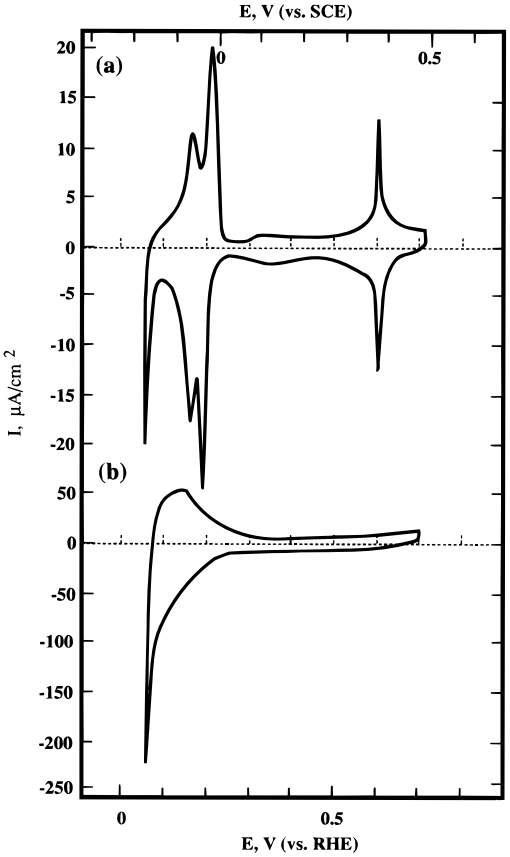

Figure 1. Cyclic voltammograms for Rh(111) in 0.01 M HF without (a) and with (b) 1 mM benzene. Scan rates were 5 and 50 mV/s for (a) and (b), respectively.

After the Rh(111) electrode was subjected to the CV measurement of Figure 1a in the pure HF solution, the electrode was transferred into a 0.01 M HF solution containing ca. 1 mM benzene. The CV indicated a featureless double-layer region between 0.3 and 0.7 V as shown in Figure 1b. The cathodic current commencing at about 0.3 V was considered to be due to simultaneous processes such as the desorption of adsorbed benzene, the adsorption of hydrogen, and the irreversible hydrogenation of benzene to cyclohexane, according to the

(22) Hallmark, V. M.; Chiang, S.; Woll, Ch. *J. Vac. Sci. Technol.* **1991**, *9*, 1111.
(23) Lippel, P. H.; Wilson, R. J.; Miller, M. D.; Chiang, S. *Phys. Rev. Lett.* **1989**, *62*, 171.
(24) Chiang, S. In *Scanning Tunneling Microscopy I* , Wiesendanger, R.; Guntherodt, H.-J., Eds.; Springer-Verlag: New York, 1991; pp 181−205.
(25) Weiss, P. S.; Eigler, D. M. *Phys. Rev. Lett.* **1993**, *71*, 3139.
(26) Wan, L.-J.; Yau, S.-L.; Swain, G. M.; Itaya, K. *J. Electroanal. Chem.* **1995,** *381*, 105.
(27) Itaya, K.; Sugawara, S.; Sashikata, K.; Furuya, N. *J. Vac. Sci. Technol.* **1990**, *A8*, 515.
(28) Honbo, H.; Sugawara, S.; Itaya, K. *Anal. Chem.* **1990**, **62**, 2424.
(29) Rhee, C. K.; Wasberg, M.; Zelenay, P.; Wieckowski, A. *Catal. Lett.* **1991**, *10*, 149.
(30) Clavilier, J.; Wasberg, M.; Petit, M.; Klein, L. H. *J. Electroanal. Chem.* **1994**. *374*, 123.

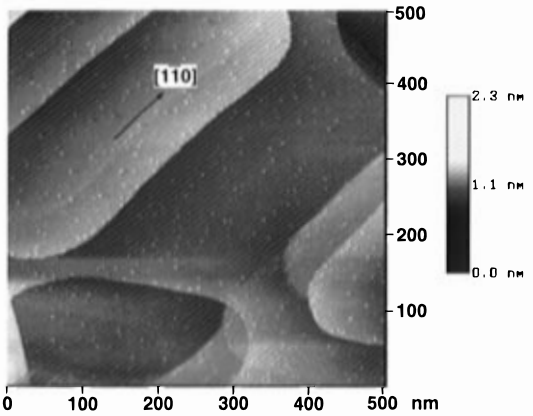

Figure 2. Topographic STM scan of a Rh(111) facet prepared by annealing and quenching. All steps are monatomic (0.23 nm in height). This image was obtained at 0.25 V with a bias voltage of 100 mV and a tunneling current of 5 nA.

previous studies using differential electrochemical mass spectrometry (DEMS).[31,32] A further anodic scan showed a peak at about 0.9 V due to the oxidation of the adsorbed benzene to CO_2.[31,32] However, the oxidation of the well-defined Rh(111) also takes place at such high potentials, resulting in surface roughening as described in our previous paper.[26] Note that the charging currents observed in the solution containing benzene decreased to about one-third of that found for the bare electrode in the pure HF solution. A similar featureless CV was also obtained with a benzene-dosed Rh(111) electrode in pure 0.01 M HF. The Rh(111) electrode was immersed in 0.01 M HF containing 1 mM benzene for 1 min at the open circuit potential and then transferred to the pure HF solution. These results strongly suggest that benzene is chemisorbed and remained on the surface of Rh(111), at least in the potential range between 0.3 and 0.7 V.

2. In Situ STM. A well-defined terrace-step structure was easily observed on the well-prepared Rh(111) face. Figure 2 shows a typical large-scale STM image acquired in an area of 500 × 500 nm^2. Only a few step lines were found in the scanned area, and atomically flat terraces usually extended over 100 nm. The well-defined steps were found to be all monatomic and aligned predominantly along the atomic rows of the Rh(111) substrate. However, some small islands were usually found on the atomically flat terraces as can be seen in Figure 2. A large number of defects such as islands and pits were sometimes observed as described previously,[11] depending on the procedure of flame-annealing−quenching.

The atomic image of Rh(111)-(1 × 1) was routinely discerned on the terrace in the pure HF solution as shown in Figure 3a. The almost perfectly aligned hexagonal structure can be seen with an interatomic distance of 0.27 nm, indicating that the structure of the Rh(111) surface has a (1 × 1) structure. Identical atomic images were consistently observed in the potential range between 0.1 and 0.75 V. No additional species were found in STM images at potentials coresponding to the butterfly peaks or the hydrogen adsorption and desorption peaks, in agreement with our previous result obtained on Rh(111) in 0.1 M $HClO_4$.[26]

After the atomic resolution shown in Figure 3a was achieved, a small amount of 1 mM benzene solution was directly added to the STM cell at 0.45 V. The average concentration of benzene in 0.01 M HF was 10 μM. Immediately after the injection of benzene, completely different patterns appeared in STM images. Figure 3b shows an example of the STM images acquired at 0.45 V. Although the small islands described in Figure 2 can be more clearly seen in the area of 25 × 25 nm^2, it is evident that the atomically flat terraces are now covered by ordered benzene adlayers. An averaged domain size was about 10 × 10 nm^2. However, the size of ordered domains was found to increase after a few potential cycles between 0.25 and 0.5 V. The image shown in Figure 3b was acquired after three potential cycles. Nevertheless, the adsorbed benzene molecules appear to form a square adlattice in each domain. Furthermore, the molecular rows in a given domain cross each other in boundaries forming an angle of either 60° or 120°.

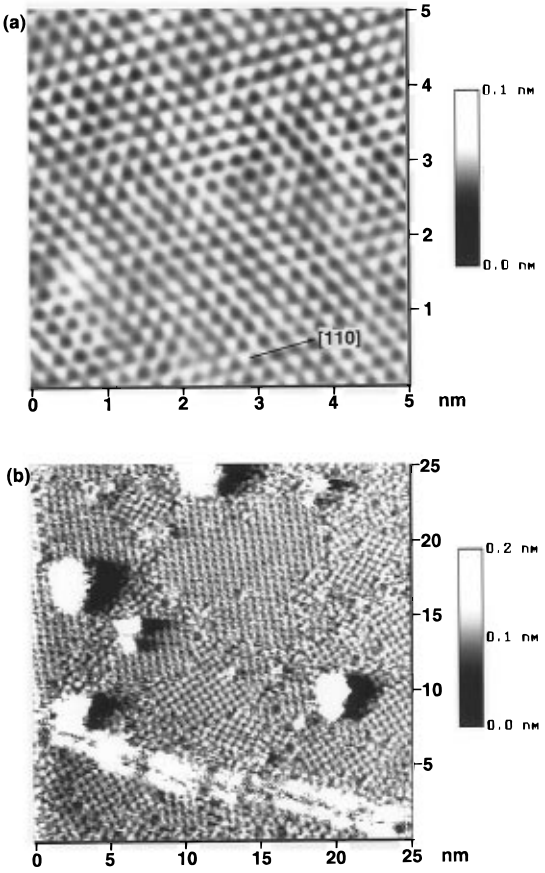

Figure 3. Atomic resolution in situ STM images of (a) Rh(111)-(1 × 1) and (b) rotational domains of the $c(2\sqrt{3} \times 3)$*rec*t benzene adlayer, respectively obtained at 0.05 and 0.45 V in 10 mM HF. The bias voltage and set-point current were 30 mV and 30 nA. (a) 2D Fourier transform filtered. (b) Unfiltered.

More details of the orientation of benzene in the adlayer were revealed by higher resolution STM images shown in Figure 4. The acquisition of these images was performed specifically under conditions with minimal thermal drift in the *x* and *y* directions in order to determine the unit cell of the adlayer as accurately as possible. Each benzene molecule usually appeared as a simple bright spot with a corrugation height of 0.07 nm as shown in Figure 4a. It is seen in Figure 4a that the molecular rows along the arrows A and B cross each other at 90°, and they are always parallel with the close-packed and $\sqrt{3}$ directions of the Rh(111) substrate, respectively. The intermolecular distances along these directions are not equal to each other and were found to be on the average 0.8 and 0.9 nm, respectively. On the basis of the orientation of molecular rows and the intermolecular distances, we concluded that the benzene adlayer was composed of rectangular unit cells, namely, $c(2\sqrt{3} \times 3)$-*rect* ($\theta = 0.17$), as shown in Figure 4a. The lattice spaces of

(31) Baltruschat, H.; Schmiemann, U. *Ber. Bunsen-Ges. Phys. Chem.* **1993**, *97*, 452.
(32) Schmiemann, U.; Jusys, Z.; Baltruschat, H. *Electrochim. Acta* **1994**, *39*, 561.

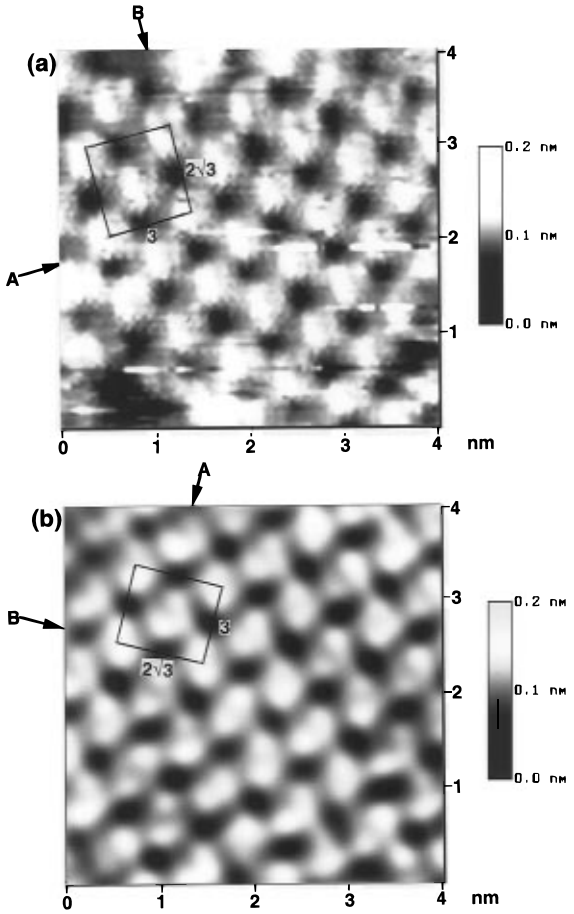

Figure 4. High-resolution in situ STM images of the $c(2\sqrt{3} \times 3)$*rect* benzene adlayer on Rh(111), acquired at 0.45 V. The images were obtained in two different areas. The markers of A and B represent the close pack and $\sqrt{3}$ directions of the Rh(111) substrate. (a) Unfiltered. (b) 2D Fourier transform filtered.

$2\sqrt{3}$ and 3 on Rh(111) (0.268 nm) correspond to 0.93 and 0.80 nm, respectively, which are consistent with our experimental values.

Surprisingly, STM images acquired with even higher resolution allowed us to determine the internal structure and microorientation of each benzene molecule adsorbed on Rh(111). The image shown in Figure 4b was acquired in a domain different from that of the image shown in Figure 3b. Although the unit cell is rotated by 60° with respect to that shown in Figure 4a, the adlayer of benzene can be defined as the $c(2\sqrt{3} \times 3)$*rect* structure. However, it is clear that each spot in the lower resolution image shown in Figure 4a is now split into two bright spots, forming a characteristic dumbbell shape for each benzene molecule. The STM discerned a 0.01 nm corrugation between the valley and ridge of each benzene molecule. It can also be seen in Figure 4b that the orientation of a dumbbell-shaped benzene is not the same as that for all molecules but depends on its positions. The dumbbell shape of the central benzene molecule in the unit cell shown in Figure 4b is clearly rotated by 60° with respect to the molecules located on the four corners of the unit cell. The molecules on the corners of the unit cell appeared with the same feature, suggesting that they sit on an identical binding site. It is also seen that the orientation of these dumbbells is always rotated by 30° with respect to the close-packed rows (arrow A in Figure 4b) of the Rh(111) substrate. Although the orientation of all benzene molecules in Figure 4b can be explained as described above, some irregularities in the array of benzene were sometimes found in the STM images, suggesting that defects were also present even in each domain.

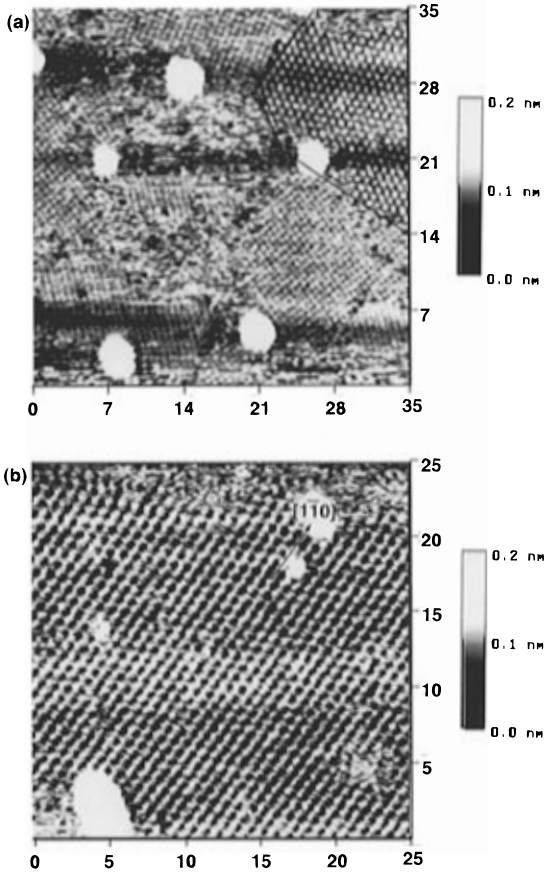

Figure 5. Unfiltered in situ STM images of (a) domain boundaries of $c(2\sqrt{3} \times 3)$*rect* and (3×3) benzene adlattices on Rh(111), the image being obtained at 0.35 V, and (b) the pure (3×3) benzene structure, obtained at 0.25 V.

The STM image shown in Figure 4b provides more detailed information on the orientation of each benzene molecule in the unit cell as discussed below.

The $c(2\sqrt{3} \times 3)$*rect* structure described above was consistently observed in the potential range between 0.4 and 0.7 V without additional structural transitions. On the other hand, it was found that the adlayer structure changed at negative potentials. A negative potential step from 0.45 to 0.35 V induced a reconstruction in the benzene adlayer from $c(2\sqrt{3} \times 3)$*rect* symmetry to an ordered hexagonal pattern. The electrode potential of 0.35 V is near the onset potential of the cathodic current as shown in Figure 1b. Figure 5 shows a set of STM images acquired in almost the same area in order to reveal the dynamic process of phase transition. It is clearly seen in Figure 5a that a new domain appeared with the hexagonal array of benzene on the upper right corner marked by solid lines, while the $c(2\sqrt{3} \times 3)$*rect* structure remained as the main phase. A further cathodic step to 0.25 V resulted in a predominantly hexagonal phase, while the $c(2\sqrt{3} \times 3)$*rect* domains were eliminated as shown in Figure 5b. This structural change occurred within a few minutes after application of the potential step. Such a long-range ordered hexagonal pattern could be seen over almost the entire area of the terrace at 0.25 V. All benzene molecules exhibited the same corrugation height of 0.07 nm, similar to that in the $c(2\sqrt{3} \times 3)$*rect* structure. The observed corrugation height depended on the STM imaging conditions including the magnitudes of tunnel current and bias voltage. A value of 0.07 nm seemed to be the maximum obtained in this study, although increasing the tunnel current led to an increase in the corrugation height. It is interesting to

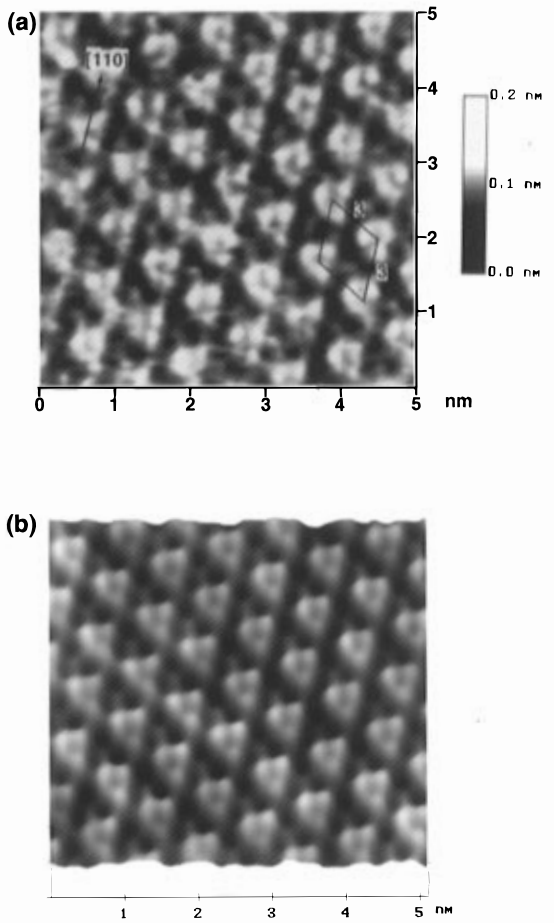

Figure 6. Unfiltered top view (a) and height-shaded plot (b) of the Rh(111)-(3 × 3)-1C_6H_6 adlattice acquired at 0.25 V in 0.05 mM benzene and 0.01 M HF. The bias voltage and feedback current were set at 30 mV and 20 nA.

note that similar values were reported for benzene on the Pt(111)[25] and Rh(111)-(3 × 3)(C_6H_6 + 2CO)[21] surfaces in UHV.

In order to reveal the internal molecular structure in the hexagonal phase, STM images were acquired under particularly carefully adjusted experimental conditions with minimal thermal drift. The images were achieved with a biased voltage of 30−100 mV and a set-point current of 20−30 nA. Figure 6a shows one of the unfiltered highest resolution images acquired on the substrate prepared differently from those used to obtain Figure 5. Compared with the crystal orientation, [110], determined by the Rh(111)-(1 × 1) atomic image, it can be seen that all benzene molecules are almost perfectly aligned along three close-packed directions of Rh(111). The molecular rows cross each other at an angle of either 60° or 120° within an experimental error of ±2°. The intermolecular distance along these rows was found to be 0.8 nm, which corresponds to 3 times the lattice parameter of Rh(111). Therefore, we conclude that the hexagonal structure is (3 × 3)-C_6H_6 ($\theta = 0.11$) as shown by the unit cell superimposed in Figure 6a. Moreover, a careful examination of the unfiltered image reveals that each benzene molecule appears as a set of three spots with similar intensity. It can also be seen that a clear dip exists in the center of each triangle with three lobes. These features can be more clearly seen in the height-shaded surface plot obtained by applying a mild 2D Fourier transform filter method as shown in Figure 6b. The spacing between the two lobes in each molecule was found to be about 0.3 nm. In addition, a weaker additional spot with a small corrugation of about 0.02 nm can be seen in the unit cell in Figure 6a. It is important to note that all these features of the STM image for the (3 × 3) adlayer observed at 0.25 V are essentially identical to those found for the coadsorbed benzene and CO adlayer on Rh(111) in UHV reported by Ohtani et al.[21] They also found the weaker spot which was attributed to the coadsorbed CO or artifacts caused by asymmetric tips.[21]

When the electrode potential was further stepped in the negative direction, the ordered (3 × 3) domain became islands with the same internal structure, suggesting that the desorption of benzene occurred preferentially at edges of the islands of ordered (3 × 3) domains. Eventually, all adsorbed benzene molecules were desorbed from the surface at 0.1 V due to the hydrogen adsorption and partially due to the hydrogenation as expected from the result obtained by DEMS,[31,32] and the Rh(111)-(1 × 1) structure, similar to that shown in Figure 3a, was consistently discerned at 0.1 V. The structural changes described above were reversible. When the electrode potential was stepped back to the positive region, the (3 × 3) and *c*(2√3 × 3)*rect* phases returned at the potentials described above.

3. Structure Models. The structures and registries of chemisorbed benzene on Rh(111) have been thoroughly scrutinized by surface sensitive techniques such as LEED, EELS, and angle-resolved UV photoemission spectroscopy (ARUPS) in UHV.[33−43] These previous studies revealed various structures for benzene, including well-known structures such as c(2√3 × 4)*rect* and (3 × 3), depending on whether CO was present unintentionally or intentionally in the UHV chambers. Although it has been repeatedly demonstrated that the adlayer structures of benzene on Rh and Pt were greatly affected by the presence of CO in the adlayer, the structure of the pure benzene adlayer has not yet been fully understood. Neuber et al. recently reported that a completely new structure with a (√19 × √19)-*R*23.4° symmetry appeared for the pure benzene adsorption on Rh(111) under cleaner UHV conditions in the absence of CO, and the previously known structures of c(2√3 × 4)*rect* and (3 × 3) were found to appear upon admission of CO.[43] We were concerned about the possibility of the existence of CO on the Rh(111) surface in HF solution. The HF solution might be expected to contain CO as an impurity from air or as a product of the electrochemical reduction of CO_2 at Rh and Pt electrodes. It is known that relatively sharp oxidation peaks appear at positive potentials on both Rh and Pt in CV when adsorbed CO exists on these electrodes.[44,45] However, it was found in this study that the anodic peak due to the oxidation of CO was hardly detectable in CV even after a prolonged STM experiment for several hours in an air-saturated HF solution. We strongly believe that the adlayer structures found in HF solution described above did not result from contamination with CO.

It is interesting to note that, in the previous study of the

(33) Mate, C. M.; Somorjai, G. A. *Surf. Sci.* **1985**, *160*, 542.
(34) Lin, R. F.; Koestner, R. J.; Van Hove, M. A.; Somorjai, G. A. *Surf. Sci.* **1983**, *134*, 161.
(35) Koel, B. E.; Crowell, J. E.; Mate, C. M.; Somorjai, G. A. *J. Phys. Chem.* **1984**, *88*, 1988.
(36) Van Hove, M. A.; Lin, R. F.; Somorjai, G. A. *J. Am. Chem. Soc.* **1986**, *108*, 2532.
(37) Ogletree, D. F.; Van Hove, M. A.; Somorjai, G. A. *Surf. Sci.* **1987**, *183*, 1.
(38) Wander, A.; Held, G.; Hwang, R. Q.; Blackman, G. S.; Xu, M. L.; Andres, P.; Van Hove, M. A.; Somorjai, G. A. *Surf. Sci.* **1991**, *249*, 21.
(39) Somorjai, G. A. *J. Phys. Chem.* **1990**, *94*, 1013.
(40) Neumann, M.; Mack, J. U.; Bertel, E.; Netzer, F. P. *Surf. Sci.* **1985**, *155*, 629.
(41) Netzer, F. P.; Rosina, G.; Bertel, E.; Saalfeld, H. *Surf. Sci.* **1987**, *184*, L397.
(42) Netzer, F. P. *Langmuir* **1991**, *7*, 2544.
(43) Neuber, M.; Schneider, F.; Zubragel, C; Neumann, M. *J. Phys. Chem.* **1995**, *99*, 9160.
(44) Hoshi, N.; Ito, H.; Suzuki, T.; Hori, Y. *J. Electroanal. Chem.* **1995**, *395*, 309.
(45) Orts, J. M.; Fernandez-Vega, A.; Feli, J. M.; Aldaz, A.; Clavilier, J. *J. Electroanal. Chem.* **1992**, *327*, 261.

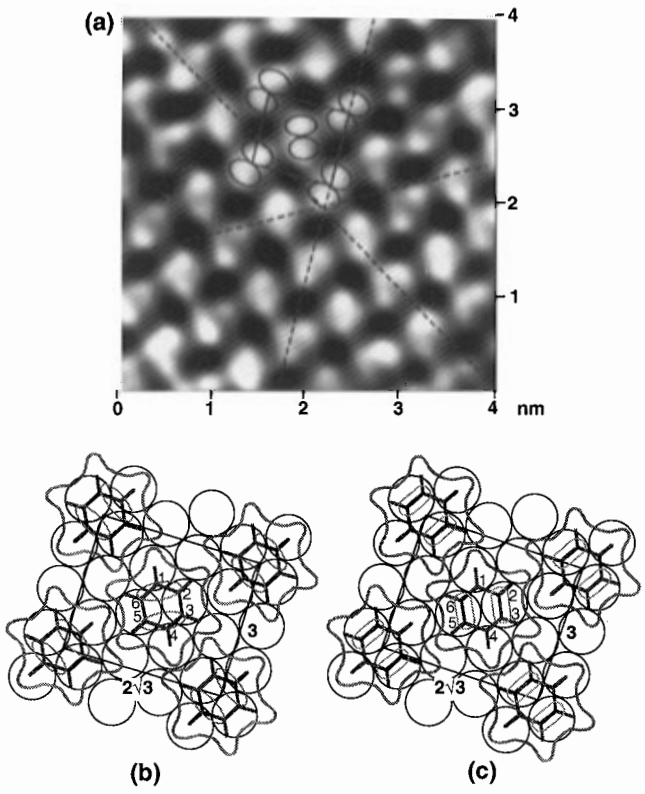

Figure 7. In situ STM image (a) of the $c(2\sqrt{3} \times 3)$*rect* structure and its real space models (b and c) for the Rh(111)-$c(2\sqrt{3} \times 3)$*rect* benzene adlattice. All benzene molecules occupy 2-fold bridging sites.

adsorbed benzene on Rh(111) in UHV,[33] one of the structures of the pure benzene adlayer was attributed to the $c(2\sqrt{3} \times 3)$-*rect* structure, which was found in solution in this study. The $c(2\sqrt{3} \times 3)$*rect* structure was also confirmed to exist by LEED on Rh(111) as a pure benzene adlayer in the above-mentioned paper by Neuber et al.[43] Nevertheless, no STM investigation in UHV has hitherto been carried out for the $c(2\sqrt{3} \times 3)$*rect* structure, although Ohtani et al. reported STM images of the coadsorbed benzene and CO with the (3×3) structure.[21]

Parts a−c of Figure 7 show the STM image reproduced from Figure 4b and the previously proposed models for the $c(2\sqrt{3} \times 3)$*rect* structure,[33] respectively. All of the adsorbed benzene molecules are assumed to be located on the 2-fold bridging sites. The benzene molecule at the center of the unit cell also occupies a 2-fold site, but it is rotated 60° from those at the corners. Weiss and Eigler reported three distinct types of STM images for isolated benzene molecules located at 3-fold hollow, atop, and bridge sites on Pt(111) at 4 K.[25] They assigned the single bump elongated perpendicularly to the bridge to the bridge-bonded benzene. In Figure 4b each benzene molecule is seen with the dumbbell shape on Rh(111) and elongated perpendicularly to the bridge. Figure 7a shows the dumbbell shape marked by a set of two split spots as well as the directions of the atomic rows of Rh(111) determined by an atomic STM image of the substrate. The solid lines in Figure 7a indicate the close-packed directions of Rh(111) determined by the STM images acquired at 0.1 V. It is more clearly seen that the directions of $2\sqrt{3}$ and 3 are rotated 30° and parallel to the atomic rows of Rh(111) within an experimental error of ±2°. It is also clear that the direction of each elongated dumbbell is always rotated approximately 30° with respect to that of the corresponding atomic row of Rh(111).

These detailed features can be explained by the model structure shown in Figure 7b, where two lobes marked by the circles are assumed to be localized near carbon atoms (1, 2, 6 and 3, 4, 5) bonded across the Rh atoms. This assumption seems to be consistent with the result obtained on Pt(111) by Weiss and Eigler[25] as described above and also with that for the (3×3) adlayer of coadsorbed benzene and CO on Rh(111) investigated by Ohtani et al.[21] Figure 7c shows the opposite situation where two lobes are assumed to be located on the carbon atoms (2, 3 and 5, 6) above the Rh atoms. It is clear that the model structure shown in Figure 7c cannot explain the microorientation of each molecule in the unit cell seen in Figure 7a. Therefore, the model shown in Figure 7b is thought to show the correct orientation.

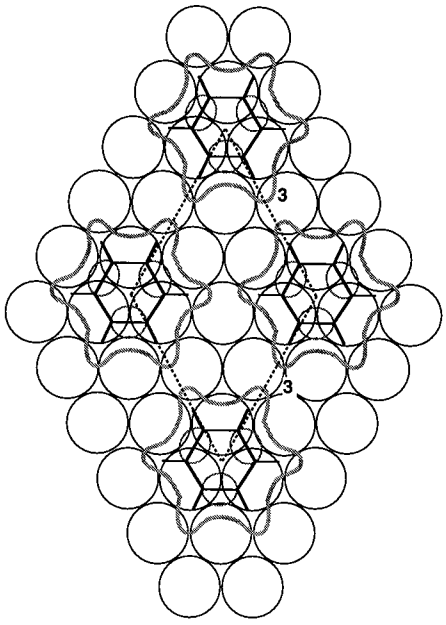

Figure 8. Real space structural model for the Rh(111)-(3×3)-$1C_6H_6$ adlattice. All molecules are assigned to 3-fold hollow sites. Each small circle between two Rh atoms represents a bright protrusion in the high-resolution STM images in Figure 6.

The STM image obtained at 0.25 V shown in Figure 5b can be explained by the structural model with (3×3) symmetry illustrated in Figure 8. Although the structure proposed here is basically the same as that proposed previously, on the basis of the LEED, EELS,[33−43] and STM[21] studies in UHV, for the adlayer of coadsorbed benzene and CO on Rh(111), two CO molecules thought to be located at the 3-fold hollow sites in the unit cell are omitted in Figure 8. Each benzene molecule is assumed to bond at the 3-fold hollow site. The coadsorption of CO was unlikely to take place in the solution under the present conditions, because no oxidation peak was observed as described above. Instead of CO, water molecules or hydronium cations might be coadsorbed near the uncoordinated 3-fold hollow sites to stabilize the (3×3) structure, their function being similar to that of the coadsorbed CO. The weaker small spots seen in Figure 6 might be due to such coadsorbed water molecules or hydronium cations. It was proposed in our previous paper that coadsorbed water molecules stabilized the adlayer of sulfate or bisulfate ions on Rh(111), and they could be clearly discerned by in situ STM.[11]

Ohtani et al. determined the benzene binding site to be hcp, rather than fcc, by STM[21] in good agreement with the previous LEED assignment,[33] while the STM image shown in Figure 6 alone cannot distinguish between the two binding sites for benzene. According to previous STM in UHV[21] and theoretical calculations,[46−48] it can be expected that the three spots for each benzene molecule as shown in Figure 6 are located between the Rh atoms as indicated by the small circles in Figure 8.

(46) Sautet, P.; Joachim, C. *Chem. Phys. Lett.* **1991**, *185*, 23−30.

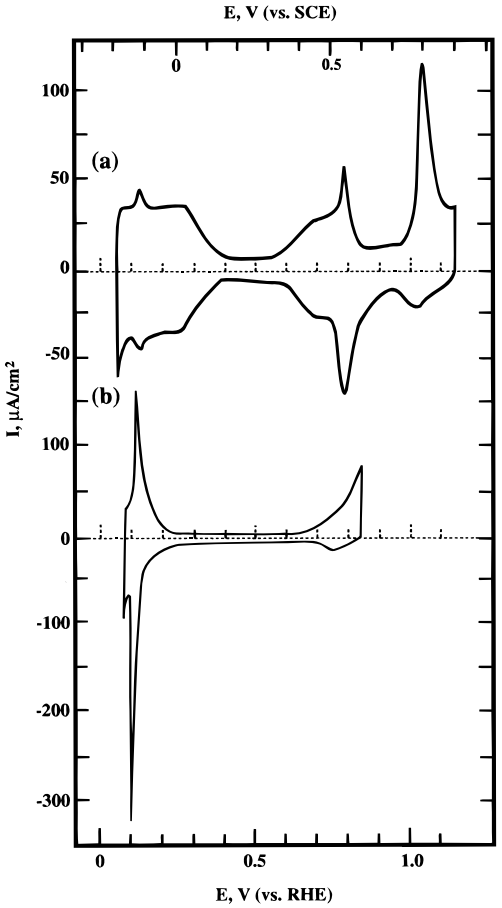

Figure 9. Cyclic voltammograms of Pt(111) in (a) 0.01 M HF and (b) 1 mM benzene + 0.01 M HF solution. The CV in (b) was recorded after three potential cycles between 0.05 and 0.8 V. The scan rate was 50 mV/s.

The surface coverage of benzene in the adlayers of $c(2\sqrt{3} \times 3)$*rect* and (3×3) are 0.17 and 0.11, respectively, indicating that a substantial amount of adsorbed benzene is desorbed from the Rh(111) surface during the potential step from 0.45 to 0.3 V. However, no clear peak corresponding to the phase transition between the two structures appears in CV in this potential range as shown in Figure 1, indicating that charge transfer processes are not involved during the adsorption and desorption of benzene in HF. The $(\sqrt{19} \times \sqrt{19})R23.4°$ ($\theta = 0.158$) structure found recently in UHV[43] might be expected to appear at potentials between 0.3 and 0.45 V, because the surface coverage of 0.158 lies between the coverages for (3×3) and $c(2\sqrt{3} \times 3)$*rect.* However, only the transformation between (3×3) and $c(2\sqrt{3} \times 3)$*rect* structures was observed in all of our experiments. The lack of the $(\sqrt{19} \times \sqrt{19})R23.4°$ structure in the solution is thought to be additional evidence that water molecules play a role in determining the adlayer structure of benzene, even though the $c(2\sqrt{3} \times 3)$*rect* structure is stable on Rh(111) both in the solution and in UHV as described above.

II. Adsorption of Benzene on Pt(111). 1. Cyclic Voltammetry. The CVs of Pt(111) in 0.01 M HF without and with 1 mM benzene are shown in parts a and b, respectively, of Figure 9. The CV shown in Figure 9a is a typical example for a well-defined Pt(111) electrode in HF that is in good agreement with previous measurements.[49] The adsorption of benzene on Pt(111) resulted in a featureless double-layer region in the potential range between 0.25 and 0.6 V. Almost reversible, sharp peaks appeared at 0.08 V just before the hydrogen evolution reaction as shown in Figure 9b. The full width at half-maximum of the cathodic peak was ca. 30 mV. These sharp peaks can be considered to be due to the adsorption and desorption of benzene on Pt(111) associated with those of hydrogen. Note that the peak height increased to a maximum value of 280 μA/cm^2 during the first five cycles and gradually decreased upon further potential cycles between 0.05 and 0.6 V. A similar complicated behavior was reported for Pt(111) in solutions containing aniline.[50] A benzene-dosed Pt(111) electrode also showed the same voltammograms in the pure HF solution during the first few cycles, while a CV identical to that shown in Figure 9a reappeared after ca. 10 cycles. However, the featureless CV was not altered by potential cycles in the limited potential range between 0.3 and 0.6 V, indicating that adsorbed benzene molecules on Pt(111) are stable in the double-layer region, but they are eliminated almost completely from the electrode surface by the potential cycle between 0.05 and 0.6 V. These results indicate that all adsorbed benzene molecules are removable from the Pt(111) surface at potentials near the hydrogen evolution potential. The anodic current starting at 0.65 V is associated with the oxidation of benzene to form CO_2 as observed by DEMS.[31,32]

2. In situ STM. The in situ STM imaging of benzene adlayers on Pt(111) was carried out in the same manner as that on Rh(111). The atomic resolution of Pt(111) substrates was firstly achieved at ca. 0.2 V within the hydrogen adsorption region before the dosing of benzene. A few drops of 1 mM benzene solution was injected usually at potentials between 0.35 and 0.6 V. The hexagonal Pt(111) lattice in the STM image was instantaneously replaced by more widely spaced, protruding features, which apparently are attributable to chemisorbed benzene molecules. It was found in this study that benzene adlayers on Pt(111) mostly appeared as less ordered phases as shown in Figure 10a than those on Rh(111) (compare with Figure 3b). However, some patches of ordered structures, for example, at the upper portion of the STM image, were unambiguously identified as ordered domains. The image was obtained at 0.35 V with a bias voltage of −65 mV and 30 nA feedback current. The intermolecular distances and directions of molecular rows indicate that the structure of the benzene adlayer at 0.35 V is $c(2\sqrt{3} \times 3)$*rect*, the same as that found on Rh(111). The degree of ordering in the $c(2\sqrt{3} \times 3)$*rect* array on Pt(111) is less than that on Rh(111), and the ordered domain size is typically 5×5 nm^2. It was not possible to acquire high-resolution STM images such as the image shown in Figure 4b to determine the orientation of each benzene molecule in the unit cell, because of a large number of defects in the adlayer. However, it was found that each molecule appeared as an elongated bump similar to that shown in Figure 4b, suggesting that all benzene molecules might be located on the bridge sites on Pt(111). The corrugation height of each molecule was ca. 0.07 nm, which was comparable to that observed on Rh(111). The benzene adlayers on Pt(111) have also previously been intensively investigated in UHV, revealing several structures including those found on Rh(111), depending on the amount of coadsorbed CO. It is interesting to note that poor ordering in the adsorbed benzene adlayer is known to occur on Pt(111) in the absence of CO in UHV.[27,38] The appearance of the disordered array on Pt(111) in HF solution seems to parallel the poor ordering observed in UHV. However, to our knowl-

(47) Garfunkel, E. L.; Minot, C.; Gavezzotti, A.; Simonetta, M. *Surf. Sci.* **1986**, *167*, 177.
(48) Anderson, A. B.; McDevitt, M. R.; Urbach, F. L. *Surf. Sci.* **1984**, *146*, 80.
(49) Wagner, F. T.; Ross, P. N. *J. Electroanal. Chem.* **1988**, *250*, 301.
(50) Albalat, R.; Claret, J.; Feliu, J. M.; Clavilier, J. *J. Electroanal. Chem.* **1990**, *288*, 277.

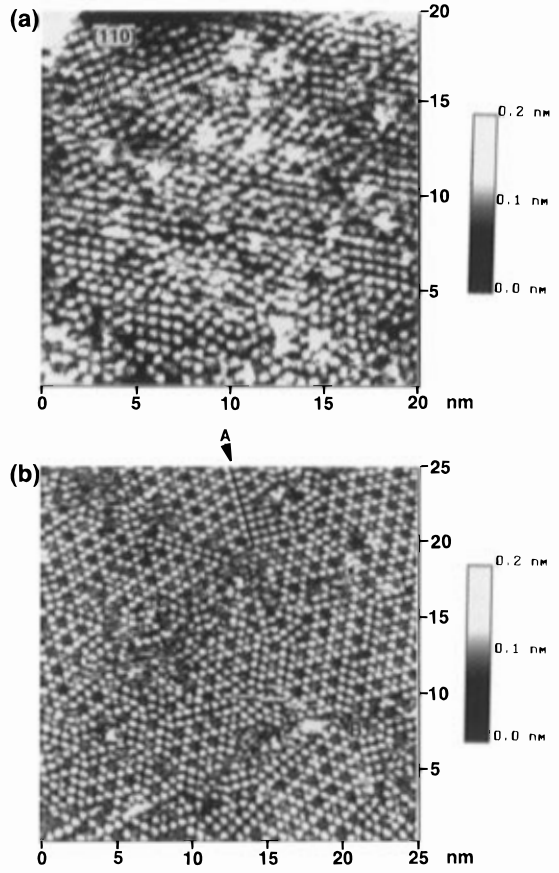

Figure 10. Unfiltered in situ STM images of (a) $c(2\sqrt{3} \times 3)$*rect*-$2C_6H_6$ and disordered benzene adlayer on Pt(111) and (b) domains of the $(\sqrt{21} \times \sqrt{21})R10.9°$-$3C_6H_6$ structure. These images were acquired at 0.35 and 0.25 V, respectively. The bias voltage and tunneling current were 60 mV and 30 nA.

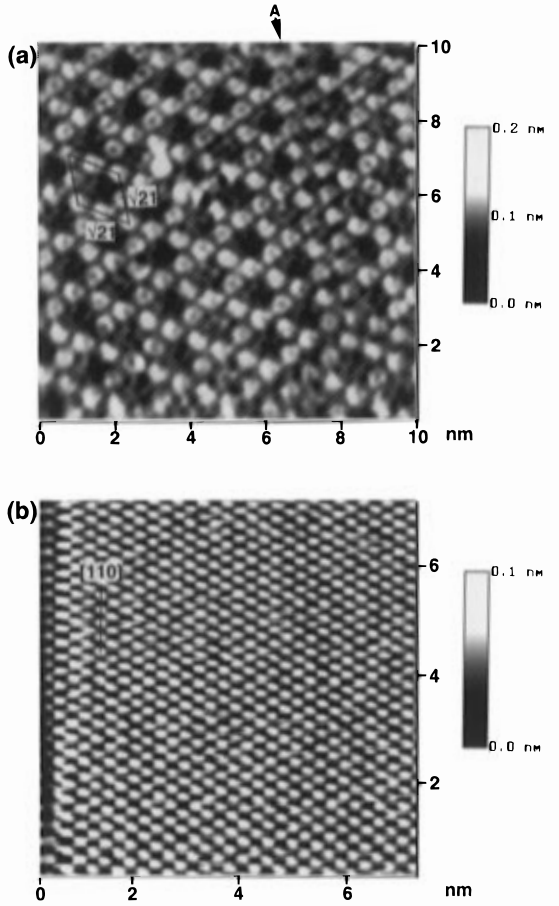

Figure 11. High-resolution STM images of (a) Pt(111)-$(\sqrt{21} \times \sqrt{21})$-$R10.9°$-$3C_6H_6$ and (b) Pt(111)-(1×1) substrate in 0.05 mM benzene and 0.01 M HF. Images were acquired at 0.25 and 0.05 V, respectively. (a) Unfiltered. (b) 2D Fourier transform filtered.

edge, the $c(2\sqrt{3} \times 3)$*rect* structure has not been reported to exist on Pt(111) in UHV.[20]

Interestingly, in situ STM revealed the reconstruction of the benzene adlayer upon the cathodic potential step from 0.35 to 0.25 V. Figure 10b shows a large-scale image of an area of 25 $\times$ 25 nm^2 obtained at 0.25 V. It is clearly seen that the adlayer is composed of highly ordered arrays with hexagonal rings, although a large number of boundaries (as indicated by markers A and B) exist between the well-ordered domains. Two types of boundaries caused by translational (marked A) and rotational (marked B) domains can be seen in the image shown in Figure 10b. All molecules seem to exhibit the same corrugation height of ca. 0.07 nm, suggesting that they are situated on the same binding site.

A closeup STM image obtained in an ordered domain is shown in Figure 11a, revealing the almost perfect array with hexagonal rings, in which only a translational domain boundary (A) can be seen. Note that some diffuse, much weaker features can also be seen inside the unit cells, presumably due to coadsorbed water molecules. We made great efforts to determine the adlayer structure as accurately as possible. After the acquisition of the image shown in Figure 11a, the electrode potential was stepped to 0.05 V, at which potential the atomic structure of Pt(111)-(1×1) was clearly observed (Figure 11b) because of the desorption of benzene as described above. The two images in Figure 11 were successively acquired upon changing the electrode potential under minimal drift. The STM image for the substrate shown in Figure 11b revealed the almost ideal hexagonal symmetry, in which the atomic rows cross each other at either 60° or 120° within a very small experimental error of ±1°. This small distortion allowed us to determine the adlayer structure observed at 0.25 V. A precise comparison of the two images revealed that the molecular rows are rotated by approximately 10° with respect to the Pt rows. The unit cell length corresponding to twice the intermolecular distance along the molecular row averages 1.26 nm, which is nearly equal to $\sqrt{21}$ times the interatomic distance of Pt (0.2778 nm). It is also evident that the molecular rows seen in Figure 11a form an angle of 60° or 120° within the experimental error.

3. Structure Models. On the basis of these detailed results, we propose that the benzene adlayer has a $(\sqrt{21} \times \sqrt{21})R10.9°$ structure ($\theta = 0.14$), whose ball models are illustrated in Figure 12. Note that this $(\sqrt{21} \times \sqrt{21})R10.9°$ structure has not previously been observed for the adsorbed benzene on Pt(111) in UHV, but it was reported on Rh(111) with coadsorbed K.[51] Figure 12 includes three possible real space structure models. The detailed structural analysis of the benzene adlayer on Pt(111) by LEED indicated that the chemisorbed benzene at 2-fold sites is greatly distorted toward the boatlike structure.[38] The two apical carbon atoms directly over the Pt atoms were found to be closer to the Pt substrate than nonapical carbons, which appeared to be bent away from the surface.[51] We tentatively adopted this orientation for benzene molecules adsorbed on Pt(111) as shown in Figure 12a on the basis of the previous LEED study mentioned above. Other sets of models could also be drawn using the orientation illustrated in Figure 7b, but they are not shown in Figure 12.

(51) Neuber, M.; Witzel, S.; Zubragel, C.; Graen, H. H.; Neumann, M. *Surf. Sci.* **1991**, *251*, 911.

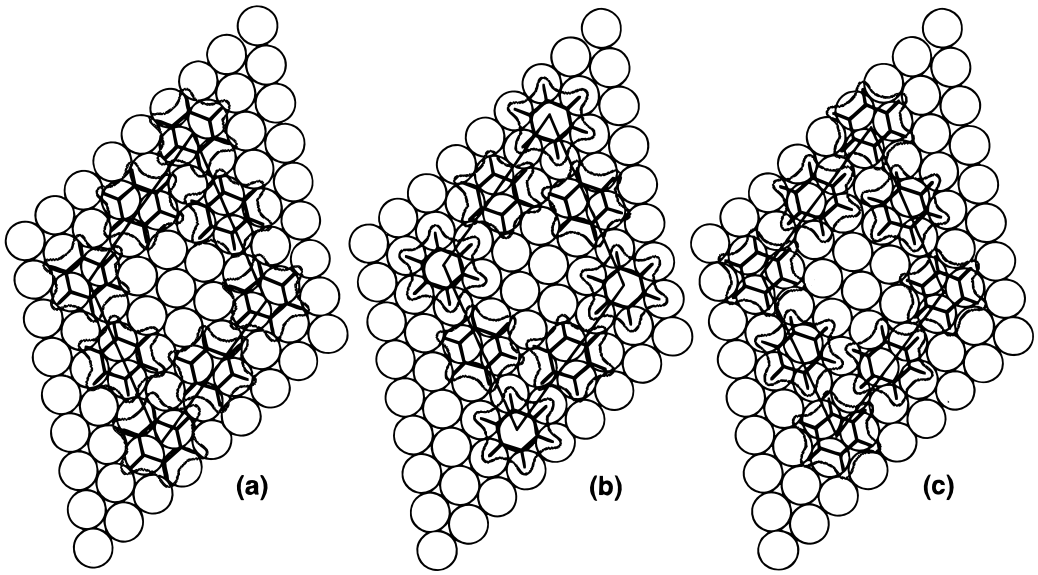

Figure 12. Three tentative ball models for Pt(111)-($\sqrt{21} \times \sqrt{21}$)*R*10.9°-3$C_6H_6$, $\theta = 0.14$. The preferred model (a) shows all benzene admolecules being assigned to 2-fold bridging sites.

All benzene molecules are located on equivalent bridge sites in the model shown in Figure 12a, whereas nonequivalent sites must be occupied by benzene in the other two cases. Four molecules at the corners of the unit cell are located on unfavorable atop sites and 3-fold hollow sites, respectively, in the models shown in Figure 12b,c. It is possible to place benzene molecules at the corners on the most favorable 3-fold sites in the third model, but the other molecules must be bound to rather unfavorable asymmetric sites. Because of the equal corrugation height observed for all benzene molecules in Figure 11a, the first model shown in Figure 12a is thought to be one of the most likely structures for ($\sqrt{21} \times \sqrt{21}$)*R*10.9°. A careful inspection of the image shown in Figure 11a might reveal alternative orientations of dumbbell-shaped or elongated benzene along the molecular rows at least in certain areas as expected from the model shown in Figure 12a, although even a higher resolution seems to be needed to determine the orientation of each molecule. It is not immediately clear why benzene molecules prefer to arrange themselves to form such an uneven structure rather than to distribute themselves uniformly to form a structure such as the (3 × 3) structure found on Rh(111). The fact that an additional benzene molecule can be squeezed into the unit cell as shown in Figure 12a can be influential to the stability of the ($\sqrt{21} \times \sqrt{21}$)*R*10.9° structure, because the additional benzene must be located on the thermodynamically unfavorable atop site. In considering the existence of coadsorbed water molecules on uncoordinated Pt atoms in the unit cell, the adsorption of hydrogen on these Pt atoms must be taken into account at the potential of 0.25 V. According to the CV obtained on the clean Pt(111) shown in Figure 9a, hydrogen adsorption is also expected to occur at 0.25 V on bare Pt atoms.

Finally, the ordered ($\sqrt{21} \times \sqrt{21}$)*R*10.9° domain became islands at more negative potentials than 0.25 V and almost abruptly disappeared at ca. 0.1 V, indicating that the desorption of adsorbed benzene takes place at edges of the islands, as was found similarly on Rh(111).

Conclusion

We presented, for the first time, high-resolution STM images of chemisorbed benzene on Rh(111) and Pt(111) electrodes in HF solution under electrochemical conditions. The presence of adsorbed benzene adlayers drastically modified the voltammetric behavior of clean Rh and Pt electrodes. In situ STM revealed the *c*($2\sqrt{3} \times 3$)*rect* ($\theta = 0.17$) structure on both Rh(111) and Pt(111) in the double-layer charging region. The degree of ordering in the *c*($2\sqrt{3} \times 3$)*rect* structure on Rh(111) was higher than that on Pt(111). Each molecule appeared as a pair of spots, suggesting that benzene is adsorbed on the 2-fold bridge site on Rh(111). The *c*($2\sqrt{3} \times 3$)*rect* structure on Rh(111) was transformed into the (3 × 3) structure, in which each molecule appeared as a triangle. The structure of the (3 × 3) adlayer observed in HF was the same as that found previously in UHV for the coadsorbed benzene and CO. However, no CO existed in the adlayer on the Rh as well as Pt surfaces in the present experimental conditions. Instead of CO, it was proposed that water molecules or hydronium cations might be adsorbed on the uncoordinated Rh atoms in the unit cell. The ($\sqrt{21} \times \sqrt{21}$)*R*10.9° ($\theta = 0.14$) adlayer was found on Pt(111) at potentials where the desorption of benzene partially took place. The high-resolution images allowed us to propose that the binding is made at 2-fold bridging sites, in the ($\sqrt{21} \times \sqrt{21}$)*R*10.9° unit cell, in which the adsorption of hydrogen was expected to occur on the uncoordinated Pt atoms. The results presented in this paper should be highly encouraging for further investigations of adsorption processes and reactions of various organic molecules on electrode surfaces in solution.

Acknowledgment. The authors acknowledge Dr. Okinaka for his help in the writing of this paper. This work was supported by the ERATO-Itaya Electrochemiscopy Project, JRDC. Y.-G.K. acknowledges support from the Korea Science and Engineering Foundation.

JA960903L